STATISTICS, OPTIMIZATION AND INFORMATION COMPUTING
Stat., Optim. Inf. Comput., Vol. **14**, October 2025, pp 1889–1908.
Published online in International Academic Press (www.IAPress.org)

On RIDS Analysis for Shade Tree Placement and Its Application to STGNN Multi-step Forecasting on RH and CO_2 Concentration of Coffee Agroforestry

Zainur Rasyid Ridlo[1,*], Dafik[2,3], Joko Waluyo[1], Yushardi[1], M. Venkatachalam[4]

[1]*Department of Science Education, University of Jember, Jember, Indonesia*
[2]*PUI-PT Combinatorics and Graph, CGANT, University of Jember, Jember, Indonesia*
[3]*Department of Mathematics, University of Jember, Jember, Indonesia*
[4]*PG and Research Department of Mathematics, Kongunadu Arts and Science College, Coimbatore-641 029, Tamil Nadu, India*

Abstract Let $G(V,E)$ be a finite, simple, and connected graph, where $|V|$ and $|E|$ denote the number of vertices and edges, respectively. A subset $D \subseteq V$ is called a dominating set if every vertex in $V \setminus D$ is adjacent to at least one vertex in D. If no two vertices in D are adjacent, then D is referred to as an independent set. The independent domination number of G, denoted by $\gamma_i(G)$, is the minimum size of an independent dominating set. For a given vertex $v \in V$, its metric representation with respect to an ordered set $W = \{w_1, w_2, \ldots, w_k\}$ is defined as the k-vector $r(v|W) = \{d(v|w_1), d(v|w_2), d(v|w_3), \ldots, d(v|w_k)\}$, where $d(v,w)$ is the shortest path distance between vertices v and w. A set W is called a resolving independent dominating set (RIDS) if it is an independent dominating set and every pair of distinct vertices in G has a unique metric representation relative to W. The smallest cardinality of such a set is known as the resolving independent domination number, denoted by $\gamma_{ri}(G)$. In this paper, we will obtain the lower and upper bounds of $\gamma_{ri}(G)$ and determine the exact value of the resolving independent domination number of some graph classes. Furthermore, to see the robust application of resolving independent domination, at the end of this paper, we will Illustrate the implementation of it on analysing Spatial Temporal Graph Neural Network (STGNN) model for multi-step forecasting on relative humidity (RH) and CO_2 concentration of coffee agroforestry.

Keywords CO_2 Concentration, Coffee Agroforestry, Relative Humidity, RIDS, Shade Tree, STGNN

AMS 2010 subject classifications 05C69, 05C85, 92D40, 68T05, 62M10

DOI: 10.19139/soic-2310-5070-2643

1. Introduction

Shade trees play a crucial role in maintaining the relative humidity and concentration of CO_2 in coffee agroforestry. This agricultural practice involves cultivating coffee plants under the canopy of taller, diverse tree species rather than in full sunlight. This method offers numerous benefits to the coffee ecosystem, environmental conservation, and the overall quality of the coffee produced. Some of their benefits are described in [1, 2, 3] and [4]. They are: *Humidity Regulation:* Shade trees help maintain optimal humidity levels in the coffee agroforestry environment. The canopy of these trees acts as a natural barrier against excessive evaporation, preventing rapid moisture loss from the soil [5]. This is particularly important in regions where coffee is grown, as maintaining consistent humidity levels is essential for the healthy growth of coffee plants; *Temperature Control:* The shade provided by the trees helps regulate the temperature in the coffee agroforestry [6, 7]. By mitigating the impact of direct sunlight, the

*Correspondence to: Zainur Rasyid Ridlo (Email: zainur.fkip@unej.ac.id). Department of Science Education, University of Jember, Jember, Indonesia.

ISSN 2310-5070 (online) ISSN 2311-004X (print)

trees create a microclimate that is cooler and more stable. This is beneficial for coffee plants, as they thrive in moderate temperatures, and it helps prevent stress and damage caused by extreme heat; CO_2 *Sequestration:* Trees are excellent carbon sinks, absorbing CO_2 from the atmosphere during photosynthesis [8, 9]. By integrating shade trees into coffee Agroforestry, farmers contribute to carbon sequestration and help offset the carbon footprint associated with agricultural activities. This is an essential aspect of sustainable and environmentally friendly coffee farming; *Biodiversity Support:* Biodiversity Support: Shade tree systems facilitate the enhancement of biodiversity by offering habitats conducive to the flourishing of diverse plant and animal species [10, 11]. The diversity of the ecosystem created by the canopy of trees encourages the presence of beneficial insects, birds, and other organisms that contribute to a balanced and healthy agricultural environment. This, in turn, reduces the need for synthetic pesticides and fosters a more sustainable and resilient ecosystem; *Soil Conservation:* The root systems of shade trees help prevent soil erosion by stabilising the soil structure[12]. This is particularly important in hilly or sloped coffee-growing regions where erosion can be a significant concern. Furthermore, trees contribute to soil health and fertility by providing organic matter to the soil through leaf litter. The illustration of shade tree in coffee Agroforestry is shown in Figure 1 and Figure 2.

Figure 1. Coffee plants with shade tree

Figure 2. Coffee plants with no shade tree

Optimal placement of shade trees using the Resolving Independent Dominating Set (RIDS) approach not only provides advantages in spatial monitoring efficiency and microclimate prediction but also carries significant ecological implications. One of them is the contribution to carbon dioxide (CO_2) sequestration from the atmosphere. Shade trees in coffee agroforestry systems have great potential as carbon sinks, depending on their species, age and distribution. Trees used in agroforestry systems show an average carbon sequestration of 2.1-4.2 tons of CO_2/ha/year [13]. In this context, tree placement based on the RIDS algorithm allows the use of a minimum number of trees with maximum coverage, thus increasing the ecological efficiency per unit of tree planted. We assume the shade tree species used have an average sequestration rate of 20 kg CO_2/tree/year [14].

The estimated annual carbon sequestration on a coffee farm with a total of 96 coffee trees having 26 shade trees is 520 kg CO_2/year, while on a grid layout with a total of 117 coffee plants having 31 shade trees is 620 kg CO_2/year. This value may seem small at a local scale, but at the scale of a large plantation, this approach can be scaled to achieve significant carbon mitigation in aggregate. Furthermore, these trees also support increased relative humidity, reduced soil temperature, and biodiversity conservation [15]. Thus, the RIDS approach is not only algorithmically efficient but also contributes to tangible ecosystem benefits. The integration of spatial dominator placement and ecological impact estimation provides a new direction for the development of AI-based smart agroforestry.

The problem is how to place the shade tree for coffee agroforestry? So far, the placement is not properly designed; see [16] and [17]. In fact, the proper placement of shade trees is crucial for their effective function in providing shade, maintaining ecological balance, and contributing to the overall health of the environment. In this study, we will use Resolving Independent Dominating Sets (RIDS) to place shade trees. It also benefits the development of control environment agriculture (CEA) technology in coffee agroforestry. The use of RIDS for the placement of shade trees also focuses on relative humidity and CO_2 monitoring by using smart sensors. RIDS involves identifying optimal locations for certain elements (in this case, shade trees) to maximise their impact on the specified objectives.

What is RIDS? We will define it in the following description. Let $G = (V, E)$ be a simple connected graph with vertex set $V(G)$ and edge set $E(G)$ [18, 19]. We define a dominating set as a set D of vertices of graph $G(V, E)$ where every vertex $u \in V(G) - D$ is adjacent to some vertex $v \in D$ [20, 21]. A set D in a graph G is known as an independent set if no two vertices within D are connected by an edge. When such a set D also serves as a dominating set, the smallest number of vertices it can contain is called the independent domination number, denoted by $\gamma_i(G)$ [22, 23, 24, 25].

In a connected graph G, the metric representation of a vertex v relative to an ordered set $W = \{w_1, w_2, w_3, \ldots, w_k\}$ of vertices in G is defined as the k-vector

$$r(v|W) = \{d(v, w_1), d(v, w_2), d(v, w_3), \ldots, d(v, w_k)\},$$

where $d(v, w)$ signifies the shortest path distance between vertices v and w.

The set W is said to be a resolving independent dominating set (RIDS) in G if it satisfies two conditions: it is an independent dominating set, and all distinct vertices in G have unique metric representations with respect to W. The least cardinality of such a set is known as the resolving independent domination number, symbolised by $\gamma_{ri}(G)$ [26].

RIDS has theoretical implications. There are a lot of relevant results that have been found, see [27] and [28]. However, the practical application of this research may not be as widespread. In this paper, we will obtain the lower and upper bounds of $\gamma_{ri}(G)$ and determine the exact value of the resolving independent domination number of some graph classes. Moreover, an analysis will be provided at the conclusion of the present document to illustrate the significant impact of resolving independent dominance. This analysis will demonstrate how this approach can be utilised in order to analyse the Spatial Temporal Graph Neural Network (STGNN) model for the multi-step forecasting of relative air humidity and CO_2 concentration in coffee agroforestry.

Spatial-Temporal Graph Neural Networks (STGNN) are a class of Graph Neural Network (GNN) models designed to handle data that exhibit both spatial and temporal dependencies within a graph structure [29, 30] and [31]. These networks are particularly useful for modeling and analyzing complex systems where entities are interconnected in both spatial and temporal dimensions [32]. STGNN have found applications in various domains, including traffic prediction, urban mobility, smart farming, climate modelling, and social network analysis; see [33, 34, 35, 36, 37] and [38]. With its ability to efficiently handle spatio-temporal dependencies, STGNN is the best approach for the prediction and classification of data involving dynamic graph structures. This model not only excels in predictive performance but also provides a deeper understanding of the interaction patterns between data in the context of space and time.

2. Method

This research uses analytical and experimental methods. In the analytical study, we used a mathematical deductive approach to obtain some theorems. The strategy used to find the new theorems is based on some known lower bounds.

Preposition 1
[27] For every graph G, we have $\gamma_{ri}(G) \geq max\{\gamma_i(G), dim(G)\}$

Theorem 1
[27] $\gamma_{ri}(P_n) = \lceil \frac{n}{3} \rceil$.

Theorem 2
[24] For two paths P_n and $P_m, \gamma_i(P_m \square P_n) \leq \lceil \frac{mn}{2} \rceil$.

However, in the experimental method, we used a computer programming language, Python, to do a simulation on STGNN multistep time series forecasting for RH and CO_2 concentrations of coffee agroforestry with the placement of shade trees in the ground using the dominant set of resolution. We place the smart sensors for relative humidity and CO_2 in the selected location of the shade trees. We will use STGNN programming to train a model of the 70% data set and test the 30% data set, and finally forecast RH and CO_2 with respect to the data collected from the smart sensors in real time. The multi-step prediction of relative humidity (RH) and CO_2 concentration in coffee agroforestry using a Graph Neural Network (GNN) follows a structured workflow. Each shade tree is treated as a node with spatial relations forming the graph edges, and sensor data as node features. This process, from graph modeling to prediction, is illustrated in Figure 3.

Single Layer GNN Algorithm

Step 0. Given that a graph $G(V, E)$ of order n and feature matrix $H_{n\times m}$ of n vertices and m features from some coffeeagroforestry, and give a tolerance ϵ.

Step 1. Determine the matrix adjacency A of graph G arising from spatiality of coffee agroforestry s and set a matrix $B = A + I$, where I is an identity matrix.

Step 2. Initialize the weight matrix W, bias β, and learning rate α. For simplicity, let $W_{m\times 1} = [w_1\, w_2 \ldots w_m]^T$ with $0 < w_j < 1$, set $\beta = 0$, and choose $0 < \alpha < 1$.

Step 3. Apply a message-passing function by multiplying the weights with node features: $\mathbf{m}_u^l = MSG^l(h_u^{l-1}) = W^l h_u^{l-1}$.

Step 4. Aggregate messages from neighbors of node v using an aggregation function: $h_v^l = AGG^l\{m_u^{l-1} \mid u \in N(v)\}$, implemented as $h_v^l = \text{SUM}^l\{m_u^{l-1} \mid u \in N(v)\}$ with respect to matrix B.

Step 5. Calculate the error: $error^l = \frac{\|h_{v_i} - h_{v_j}\|_2}{|E|}$, where v_i and v_j are any two connected nodes.

Step 6. Check if $error \leq \epsilon$. If true, terminate the algorithm. Otherwise, proceed to update the weights in Step 7.

Step 7. Update the weights using the rule: $W^{l+1} = W_j^l - \alpha \cdot z_j \cdot e^l$, where z_j is the mean of the j-th column of $H_{v_i}^l$.

Step 8. Save the resulting embeddings into a vector. If working with time series data, repeat the entire process for the next time step.

Step 9. Load the embedding vectors and apply time series machine learning techniques for training, testing, and performing multi-step forecasting.

Step 10. If the RMSE is less than or equal to ϵ, stop. Otherwise, adjust W and repeat Steps 2 through 9.

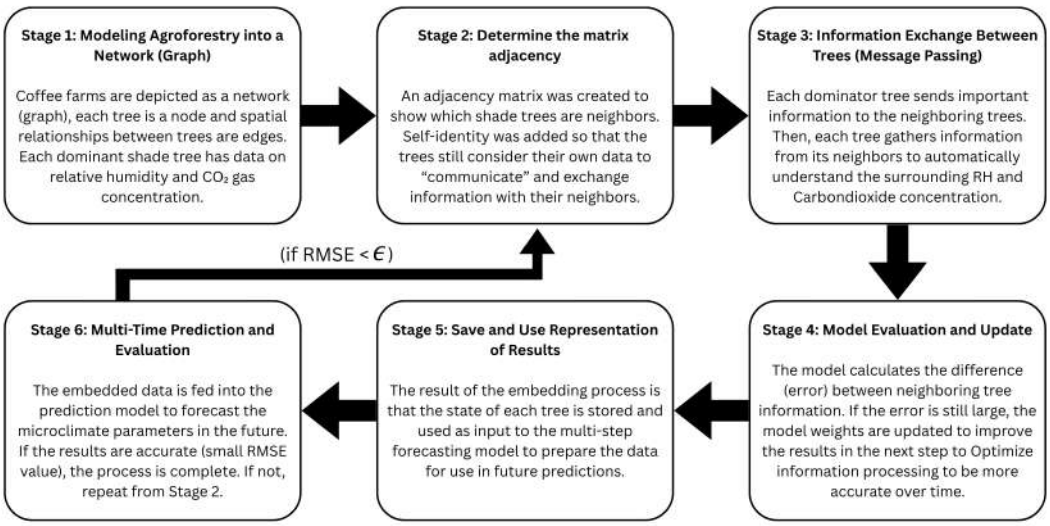

Figure 3. Simple Step Single Layer GNN Algorithm

3. Main Result

3.1. Resolving Independent Dominating Set

In this section, we will show the existence of a resolving independent dominating set of some graphs, and determine the exact value of the resolving independent domination number of $C_m \triangleright P_n$ and the grid graph. Further, we will use the obtained theorem for analysing the STGNN model for autonomous Controlled Environment Agriculture (CEA) development on multi-step time series forecasting for relative humidity and CO_2 concentration of coffee agroforestry.

Theorem 3
Let $C_m \triangleright P_n$ be a comb product of C_m and P_n graphs of $m \geq 3, n \geq 2$. We have the following:

$$\gamma_{ri}(C_m \triangleright P_n) = \begin{cases} \left\lceil \frac{n}{3} \right\rceil m & \text{for } m \geq 3, n \equiv 2(mod\ 3), n \geq 2 \\ \frac{mn}{3} & \text{for } m \geq 3, n \equiv 0(mod\ 3) n \geq 2 \\ \left\lceil \frac{m}{2} \right\rceil \left\lfloor \frac{n}{3} \right\rfloor + \left\lfloor \frac{m}{2} \right\rfloor \left\lceil \frac{n}{3} \right\rceil & \text{for } m \equiv 1(mod\ 2), m \geq 3, n \equiv 1(mod\ 3), n \geq 2 \\ \frac{n}{2}\left(\left\lfloor \frac{n}{3} \right\rfloor + \left\lceil \frac{n}{3} \right\rceil\right) & \text{for } m \equiv 0(mod\ 2), m \geq 3, n \equiv 1(mod\ 3), n \geq 2. \end{cases}$$

Proof. Comb product $C_m \triangleright P_n$ is a connected graph with vertex set $V(C_m \triangleright P_n) = \{x_{i,j}; 1 \leq i \leq m, 1 \leq j \leq n\}$ and edge set $E(C_m \triangleright P_n) = \{x_{i,j}x_{i,j+1}; 1 \leq i \leq m, 1 \leq j \leq n-1\} \cup \{x_{i,1}x_{i+1,1}; 1 \leq i \leq m-1\} \cup \{x_{i,1}x_{m,1}\}$. The cardinality of the vertex set $C_m \triangleright P_n$ is mn, and the cardinality of the edges set $C_m \triangleright P_n$ is mn. To prove the resolving independent domination number of $C_m \triangleright P_n$, we split it into four cases.

Case 1. $m \geq 3, n \equiv 2(mod\ 3), n \geq 2$
For this case, we define a subset D into two subcases. For $m \equiv 0(mod\ 2), n \equiv 2(mod\ 3), n \geq 2$, we define a

subset $D = \{x_{i,j}; i \equiv 1(mod\ 2), 1 \leq i \leq m-1, j \equiv 1(mod\ 3), 1 \leq j \leq n\} \cup \{x_{i,j}; i \equiv 0(mod\ 2), 2 \leq i \leq m, j \equiv 0(mod\ 3), 1 \leq j \leq n-2\} \cup \{x_{i,j}; i \equiv 0(mod\ 2), 2 \leq i \leq m, j = n\}$. For $m \equiv 1(mod\ 2), n \equiv 2(mod\ 3), n \geq 2$, we define a subset $D = \{x_{i,j}; i \equiv 1(mod\ 2), 1 \leq i \leq m-1, j \equiv 1(mod\ 3), 1 \leq j \leq n\} \cup \{x_{i,j}; i \equiv 0(mod\ 2, 2 \leq i \leq m-1, j \equiv 0(mod\ 3), 1 \leq j \leq n-2\} \cup \{x_{i,j}; i \equiv 0(mod\ 2), 2 \leq i \leq m-1, j = n\} \cup \{x_{i,j}; i = n, j \equiv 0(mod\ 3, 1 \leq j \leq n-2\} \cup \{x_{i,j}; i = n, j \equiv 0(mod\ 3, j = n\}$. Based on this subset, we have $|D| = \lceil \frac{n}{3} \rceil m$. Further, we will show that for any two vertices $x_{i,j}, x_{k,l} \in D$, the distance $d(x_{i,j}, x_{k,l}) \geq 2$. It implies that for any two dominators that are not adjacent to each other. It is an independent dominating set. Moreover, we need to show that the subset D complies with the resolving set properties, namely each vertex $x_{i,j} \in V(C_m \triangleright P_n)$ has a different representation with respect to D. To show that the subset of distances from each vertex to the dominators is distinct, we develop some distance function written after Case 4. Based on this function, the subset D satisfies the resolving set criterion. The last, we need to prove that the cardinality of D is the smallest one. Suppose the least $|D| = \lceil \frac{n}{3} \rceil m - 1$, thus there is $x_{m,n} \notin D$ which is not dominated by D. It concludes that $\gamma_{ri}(C_m \triangleright P_n) = \lceil \frac{n}{3} \rceil m$ for $m \geq 3, n \equiv 2(mod\ 3), n \geq 2$.

Case 2. $m \geq 3, n \equiv 0(mod\ 3) n \geq 2$

For this case, we define a subset $D = \{x_{i,j}; 1 \leq i \leq m, j \equiv 2(mod\ 3), 1 \leq j \leq n\}$. Based on this subset, we have $|D| = \frac{mn}{3}$. Further, we will show that for any two vertices $x_{i,j}, x_{k,l} \in D$, the distance $d(x_{i,j}, x_{k,l}) \geq 2$. It implies that for any two dominators that are not adjacent to each other. It is an independent dominating set. Moreover, we need to show that the subset D complies with the resolving set properties, namely each vertex $x_{i,j} \in V(C_m \triangleright P_n)$ has a different representation with respect to D. To establish the uniqueness of a subset's representation, we utilize the distance function to calculate the distance from each vertex to a dominator, see the function after Case 4. Based on this function, the subset D satisfies the resolving set criterion. The last, we need to prove that the cardinality of D is the smallest one. Suppose $|D| = \frac{mn}{3} - 1$ is the minimum one, thus there are $x_{m,n}, x_{m,n-1}, x_{m,n-2} \notin D$ which is not dominated by D. It concludes that $\gamma_{ri}(C_m \triangleright P_n) = \frac{mn}{3}$ for $m \geq 3, n \equiv 0(mod\ 3) n \geq 2$.

Case 3. $m \equiv 1(mod\ 2), m \geq 3, n \equiv 1(mod\ 3), n \geq 2$

For this case, we define a subset $D = \{x_{i,j}; i \equiv 1(mod\ 2), 1 \leq i \leq m-2, j \equiv 0(mod\ 3), 1 \leq j \leq n-1\} \cup \{x_{i,j}; i \equiv 0(mod\ 2), 2 \leq i \leq m-1, j \equiv 1(mod\ 3), 1 \leq j \leq n\} \cup \{x_{i,j}; i = m, j \equiv 0(mod\ 3, 1 \leq j \leq n-1\}$.
Based on this subset, we have $|D| = \lceil \frac{m}{2} \rceil \lfloor \frac{n}{3} \rfloor + \lfloor \frac{m}{2} \rfloor \lceil \frac{n}{3} \rceil$. Further, we will show that for any two vertices $x_{i,j}, x_{k,l} \in D$, the distance $d(x_{i,j}, x_{k,l}) \geq 2$. It implies that for any two dominators that are not adjacent to each other. It is an independent dominating set. Moreover, we need to show that the subset D complies with the resolving set properties, namely each vertex $x_{i,j} \in V(C_m \triangleright P_n)$ has a different representation with respect to D. To establish the uniqueness of a subset's representation, we utilize the distance function to calculate the distance from each vertex to a dominator, see the function after Case 4. Based on this function, the subset D satisfies the resolving set criterion. The last, we need to prove that the cardinality of D is the smallest one. Suppose $|D| = \lceil \frac{m}{2} \rceil \lfloor \frac{n}{3} \rfloor + \lfloor \frac{m}{2} \rfloor \lceil \frac{n}{3} \rceil - 1$ is the minimum one, thus there are $x_{m,n}, x_{m,n-1}, x_{m,n-2} \notin D$ which is not dominated by D. It concludes that $\gamma_{ri}(C_m \triangleright P_n) = \lceil \frac{m}{2} \rceil \lfloor \frac{n}{3} \rfloor + \lfloor \frac{m}{2} \rfloor \lceil \frac{n}{3} \rceil$ for $m \equiv 1(mod\ 2), m \geq 3, n \equiv 1(mod\ 3), n \geq 2$.

Case 4. $m \equiv 0(mod\ 2), m \geq 3, n \equiv 1(mod\ 3), n \geq 2$

For this case, we define a subset $D = \{x_{i,j}; i \equiv 1(mod\ 2), 1 \leq i \leq m-1, j \equiv 0(mod\ 3), 1 \leq j \leq n\} \cup \{x_{i,j}; i \equiv 0(mod\ 2), 2 \leq i \leq m, j \equiv 1(mod\ 3), 1 \leq j \leq n\}$. Based on this subset, we have $|D| = \frac{n}{2} \left(\lfloor \frac{n}{3} \rfloor + \lceil \frac{n}{3} \rceil \right)$. Further, we will show that for any two vertices $x_{i,j}, x_{k,l} \in D$, the distance $d(x_{i,j}, x_{k,l}) \geq 2$. It implies that for any two dominators that are not adjacent to each other. It is an independent dominating set. Moreover, we need to show that the subset D complies with the resolving set properties, namely each vertex $x_{i,j} \in V(C_m \triangleright P_n)$ has a different representation with respect to D. To establish the uniqueness of a subset's representation, we utilize the distance function to calculate the distance from each vertex to a dominator, see the function after Case 4. Based on this function, the subset D satisfies the resolving set criterion. The last, we need to prove that the cardinality of D is the smallest one. Suppose the least $|D| = \frac{n}{2} \left(\lfloor \frac{n}{3} \rfloor + \lceil \frac{n}{3} \rceil \right) - 1$, thus there are $x_{m,n}, x_{m,n-1} \notin D$ which is not dominated by D. It concludes that $\gamma_{ri}(C_m \triangleright P_n) = \frac{n}{2} \left(\lfloor \frac{n}{3} \rfloor + \lceil \frac{n}{3} \rceil \right)$ for $m \equiv 0(mod\ 2), m \geq 3, n \equiv 1(mod\ 3), n \geq 2$.

Based on Case 1 - Case 4, we can write the distance function of any two vertices in the following: $d(x_{i,j}x_{k,l}) = \begin{cases} |j-l| & \text{if } i = k \\ |i-k|+|j-l| & \text{if } i \neq k. \end{cases}$ For illustration of the resolving independent dominating set, it can be seen in Figure 4. The distance representation of the graph $C_5 \triangleright P_3$ can be written in Table 1.

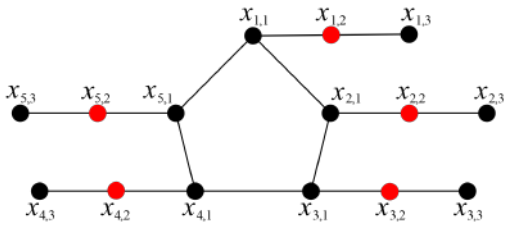

Figure 4. The Illustration of resolving independent dominating set of $C_5 \triangleright P_3$

Table 1. The distance representation $x_{i,j} \in C_5 \triangleright P_3$ to $W = \{x_{1,2}, x_{2,2}, x_{3,2}, x_{4,2}, x_{5,2}\}$

$x_{i,j}$	$r(x_{i,j}\|W)$	$x_{i,j}$	$r(x_{i,j}\|W)$	$x_{i,j}$	$r(x_{i,j}\|W)$
$x_{1,1}$	$(1,2,3,3,2)$	$x_{2,3}$	$(4,1,4,5,5)$	$x_{4,2}$	$(4,4,3,0,3)$
$x_{1,2}$	$(0,3,4,4,3)$	$x_{3,1}$	$(3,2,1,2,3)$	$x_{4,3}$	$(5,5,4,1,4)$
$x_{1,3}$	$(1,4,5,5,4)$	$x_{3,2}$	$(4,3,0,3,4)$	$x_{5,1}$	$(2,3,3,2,1)$
$x_{2,1}$	$(2,1,2,3,3)$	$x_{3,3}$	$(5,4,1,4,5)$	$x_{5,2}$	$(3,4,4,3,0)$
$x_{2,2}$	$(3,0,3,4,4)$	$x_{4,1}$	$(3,3,2,1,2)$	$x_{5,3}$	$(4,5,5,4,1)$

Theorem 4
Let $G_{m,n}$ be a grid graph with $m \geq 3, n \geq 3$. We have the following:

$$\gamma_{ri}(G_{m,n}) = \begin{cases} \lceil \frac{n}{2} \rceil \frac{m}{4} + \lfloor \frac{n}{2} \rfloor (\frac{m}{4}+1) & \text{for } m \equiv 0(mod\ 4), n \equiv 1(mod\ 2), n \geq 3 \\ \frac{mn}{4} & \text{for } m \equiv 0(mod\ 4), n \equiv 0(mod\ 2), n \geq 3 \\ \lceil \frac{n}{2} \rceil \lfloor \frac{m}{4} \rfloor + \lfloor \frac{n}{2} \rfloor \lceil \frac{m}{4} \rceil & \text{for } m \equiv 1(mod\ 4), n \geq 3 \\ \lceil \frac{m}{4} \rceil n & \text{for } m \equiv 2(mod\ 4), n \equiv 1(mod\ 2), n \geq 3 \\ & \text{for } m \equiv 2(mod\ 4), m \not\equiv 0,4(mod\ 10), n \equiv 0(mod\ 2) \\ & \text{for } m \equiv 3(mod\ 4), n \geq 3 \\ \frac{n}{2}\left(\lfloor \frac{m}{3} \rfloor + \lceil \frac{m}{5} \rceil \right) & \text{for } m \equiv 2(mod\ 4), m \equiv 0,4(mod\ 10), n \equiv 0(mod\ 2) \end{cases}.$$

Proof. Grid graph $G_{n,m}$ is a connected graph with vertex set $V(G_{m,n}) = \{x_{i,j}; 1 \leq i \leq n, 1 \leq j \leq m\}$ and edge set $E(G_{m,n}) = \{x_{i,j}x_{i,j+1}; 1 \leq i \leq n, 1 \leq j \leq m-1\} \cup \{x_{i,j}x_{i+1,j}; 1 \leq i \leq n-1, 1 \leq j \leq m\}$. Thus, the order and size of $(G_{n,m})$ are $|V(G_{m,n})| = mn$ and $|E(G_{m,n})| = 2mn - m - n$. To prove this theorem, we split it into several cases.

Case 1. $m \equiv 0(mod\ 4), n \equiv 1(mod\ 2), n \geq 3$
For this case, we define a subset $D = \{x_{i,j}; i \equiv 1(mod\ 2), j \equiv 3(mod\ 4), 1 \leq i \leq n, 1 \leq j \leq m\} \cup \{x_{i,j}; i \equiv 0(mod\ 2), j \equiv 1(mod\ 4), 1 \leq i \leq n, 1 \leq j \leq m-3\} \cup \{x_{i,j}; i \equiv 0(mod\ 2), j = m\}$. Based on this subset, we have $|D| = \lceil \frac{n}{2} \rceil \frac{m}{4} + \lfloor \frac{n}{2} \rfloor \left(\frac{m}{4}+1\right)$. Further, we will show that this subset satisfies the the resolving independent dominating set of $G_{n,m}$. We find that for any two vertices $x_{i,j}, x_{k,l} \in D$, the distance $d(x_{i,j}, x_{k,l}) \geq 2$. It implies that for any two dominators are not adjacent each other. It is independent dominating set. Moreover, we need to show that the subset D complies the resolving set properties, namely each vertex $v \in V(G)$ has different representation with respect to D. To establish the uniqueness of a subset's representation, we utilize the distance function to calculate the distance from each vertex to a dominator, see the function after Case 6. Based on this function, the subset D satisfies the resolving set criterion. The last, we need to prove that the

cardinality of D is the smallest one. Suppose $|D| = \lceil \frac{n}{2} \rceil \frac{m}{4} + \lfloor \frac{n}{2} \rfloor (\frac{m}{4} + 1) - 1$ is the minimum one, thus there are $x_{m,n-1}, x_{m,n-2} \notin D$ which is not dominated by D. It concludes that $\gamma_{ri}(G_{m,n}) = \left\lceil \frac{n}{2} \right\rceil \frac{m}{4} + \left\lfloor \frac{n}{2} \right\rfloor \left(\frac{m}{4} + 1\right)$ for $m \equiv 0(mod\ 4), n \equiv 1(mod\ 2), n \geq 3$.

Case 2. $m \equiv 0(mod\ 4), n \equiv 0(mod\ 2), n \geq 3$
For this case, we define a subset $D = \{x_{i,j}; i \equiv 1(mod\ 4), j \equiv 2(mod\ 4) 1 \leq j \leq m-2\} \cup \{x_{i,j}; i \equiv 2(mod\ 4), j \equiv 0(mod\ 4) 1 \leq j \leq m\} \cup \{x_{i,j}; i \equiv 3(mod\ 4), j \equiv 1(mod\ 4) 1 \leq j \leq m-3\} \cup \{x_{i,j}; i \equiv 0(mod\ 4), j \equiv 3(mod\ 4) 1 \leq j \leq m-1\}$. Based on this subset, we have $|D| = \frac{mn}{4}$. Further, we will show that this subset satisfies the resolving independent dominating set of $G_{n,m}$. We find that for any two vertices $x_{i,j}, x_{k,l} \in D$, the distance $d(x_{i,j}, x_{k,l}) \geq 2$. It implies that for any two dominators are not adjacent each other. It is independent dominating set. Moreover, we need to show that the subset D complies the resolving set properties, namely each vertex $v \in V(G)$ has different representation with respect to D. To establish the uniqueness of a subset's representation, we utilize the distance function to calculate the distance from each vertex to a dominator, see the function after Case 6. Based on this function, the subset D satisfies the resolving set criterion. The last, we need to prove that the cardinality of D is the smallest one. Suppose $|D| = \frac{mn}{4} - 1$ is the minimum one, thus there is $x_{i,j} \notin D$ which is not dominated by D. It concludes that $\gamma_{ri}(G_{m,n}) = \frac{mn}{4}$ for $m \equiv 0(mod\ 4), n \equiv 0(mod\ 2), n \geq 3$.

Case 3. $m \equiv 1(mod\ 4), n \geq 3$
For this case, we define a subset $D = \{x_{i,j}, i \equiv 1(mod\ 2), j \equiv 3(mod\ 4), 1 \leq i \leq n, 1 \leq j \leq m-2\} \cup \{x_{i,j}, i \equiv 0(mod\ 2), j \equiv 1(mod\ 4), 1 \leq i \leq n, 1 \leq j \leq m\}$. Based on this subset, we have $|D| = \left\lceil \frac{n}{2} \right\rceil \left\lfloor \frac{m}{4} \right\rfloor + \left\lfloor \frac{n}{2} \right\rfloor \left\lceil \frac{m}{4} \right\rceil$. Further, we will show that this subset satisfies the resolving independent dominating set of $G_{n,m}$. We find that for any two vertices $x_{i,j}, x_{k,l} \in D$, the distance $d(x_{i,j}, x_{k,l}) \geq 2$. It implies that for any two dominators are not adjacent each other. It is independent dominating set. Moreover, we need to show that the subset D complies the resolving set properties, namely each vertex $v \in V(G)$ has different representation with respect to D. To establish the uniqueness of a subset's representation, we utilize the distance function to calculate the distance from each vertex to a dominator, see the function after Case 6. Based on this function, the subset D satisfies the resolving set criterion. The last, we need to prove that the cardinality of D is the smallest one. Suppose $|D| = \frac{mn}{4} - 1$ is the minimum one, thus there is $x_{i,j} \notin D$ which is not dominated by D. It concludes that $\gamma_{ri}(G_{m,n}) = \left\lceil \frac{n}{2} \right\rceil \left\lfloor \frac{m}{4} \right\rfloor + \left\lfloor \frac{n}{2} \right\rfloor \left\lceil \frac{m}{4} \right\rceil$ for $m \equiv 1(mod\ 4), n \geq 3$.

Case 4. $m \equiv 2(mod\ 4), n \equiv 1(mod\ 2), n \geq 3$ and $m \equiv 2(mod\ 4), m \not\equiv 0, 4(mod\ 10), n \equiv 0(mod\ 2)$
For this case, we define a subset $D = \{x_{i,j}; i \equiv 1(mod\ 2), j \equiv 3(mod\ )4, 1 \leq i \leq n, 1 \leq j \leq m-3\} \cup \{x_{i,m}; i \equiv 1(mod\ 2), 1 \leq i \leq n\} \cup \{x_{i,j}; i \equiv 0(mod\ 2), j \equiv 1(mod\ 4), 1 \leq i \leq n, 1 \leq j \leq m-1\}$. Based on this subset, we have $|D| = \lceil \frac{m}{4} \rceil n$ Further, we will show that this subset satisfies the resolving independent dominating set of $G_{n,m}$. We find that for any two vertices $x_{i,j}, x_{k,l} \in D$, the distance $d(x_{i,j}, x_{k,l}) \geq 2$. It implies that for any two dominators are not adjacent each other. It is independent dominating set. Moreover, we need to show that the subset D complies the resolving set properties, namely each vertex $v \in V(G)$ has different representation with respect to D. To establish the uniqueness of a subset's representation, we utilize the distance function to calculate the distance from each vertex to a dominator, see the function after Case 6. Based on this function, the subset D satisfies the resolving set criterion. The last, we need to prove that the cardinality of D is the smallest one. Suppose $|D| = \left\lceil \frac{m}{4} \right\rceil n - 1$ is the minimum one, thus there is $x_{i,j} \notin D$ which is not dominated by D. It concludes that $\gamma_{ri}(G_{m,n}) = \left\lceil \frac{m}{4} \right\rceil n$ for $m \equiv 2(mod\ 4), n \equiv 1(mod\ 2), n \geq 3$.

Case 5. $m \equiv 3(mod\ 4), n \geq 3$
For this case, we define a subset $D = \{x_{i,j}; i \equiv 1(mod\ 2), j \equiv 3(mod\ 2), 1 \leq i \leq n, 1 \leq j \leq m\} \cup \{i \equiv 0(mod\ 2), j \equiv 1(mod\ 4), 1 \leq i \leq n, 1 \leq j \leq m-2\}$. Based on this subset, we have $|D| = \lceil \frac{m}{4} \rceil n$ Further, we will show that this subset satisfies the resolving independent dominating set of $G_{n,m}$. We find that for any two vertices $x_{i,j}, x_{k,l} \in D$, the distance $d(x_{i,j}, x_{k,l}) \geq 2$. It implies that for any two dominators are not adjacent each other. It is independent dominating set. Moreover, we need to show that the subset D complies the resolving set properties, namely each vertex $v \in V(G)$ has different representation with respect to D. To establish the uniqueness of a subset's representation, we utilize the distance function to calculate the distance from each vertex to a dominator, see the function after Case 6. Based on this function, the subset D satisfies the resolving set criterion. The last, we

need to prove that the cardinality of D is the smallest one. Suppose $|D| = \lceil \frac{m}{4} \rceil n - 1$ is the minimum one, thus there is $x_{i,j} \notin D$ which is not dominated by D. It concludes that $\gamma_{ri}(G_{m,n}) = \lceil \frac{m}{4} \rceil n$ for $m \equiv 3(mod\ 4), n \geq 3$.

Case 6. $m \equiv 2(mod\ 4), m \equiv 0, 4(mod\ 10), n \equiv 0(mod\ 2)$

For this case, we define a subset $D = \{x_{i,j}; i \equiv 1(mod\ 4), j \equiv 2(mod\ 10)\} \cup \{x_{i,j}; i \equiv 1(mod\ 4), j \equiv 6(mod\ 10)\} \cup \{x_{i,j}; i \equiv 1(mod\ 4), j \equiv 8(mod\ 10)\} \cup \{x_{i,j}; i \equiv 2(mod\ 4), j \equiv 0(mod\ 10)\} \cup \{x_{i,j}; i \equiv 2(mod\ 4), j \equiv 4(mod\ 10)\} \cup \{x_{i,j}; i \equiv 3(mod\ 4), j \equiv 1(mod\ 10)\} \cup \{x_{i,j}; i \equiv 3(mod\ 4), j \equiv 7(mod\ 10)\} \cup \{x_{i,j}; i \equiv 0(mod\ 4), j \equiv 3(mod\ 10)\} \cup \{x_{i,j}; i \equiv 0(mod\ 4), j \equiv 5(mod\ 10)\} \cup \{x_{i,j}; i \equiv 0(mod\ 4), j \equiv 9(mod\ 10)\}$. Based on this subset, we have $|D| = \frac{n}{2}\left(\lfloor \frac{m}{3} \rfloor + \lceil \frac{m}{5} \rceil\right)$. Further, we will show that this subset satisfies the resolving independent dominating set of $G_{n,m}$. We find that for any two vertices $x_{i,j}, x_{k,l} \in D$, the distance $d(x_{i,j}, x_{k,l}) \geq 2$. It implies that for any two dominators are not adjacent each other. It is independent dominating set. Moreover, we need to show that the subset D complies the resolving set properties, namely each vertex $v \in V(G)$ has different representation with respect to D. To establish the uniqueness of a subset's representation, we utilize the distance function to calculate the distance from each vertex to a dominator, see the function after Case 6. Based on this function, the subset D satisfies the resolving set criterion. The last, we need to prove that the cardinality of D is the smallest one. Suppose $|D| = \frac{n}{2}\left(\lfloor \frac{m}{3} \rfloor + \lceil \frac{m}{5} \rceil\right) - 1$ is the minimum one, thus there is $x_{i,j} \notin D$ which is not dominated by D. It concludes that $\gamma_{ri}(G_{m,n}) = \frac{n}{2}\left(\lfloor \frac{m}{3} \rfloor + \lceil \frac{m}{5} \rceil\right)$ for $m \equiv 2(mod\ 4), m \equiv 0, 4(mod\ 10), n \equiv 0(mod\ 2)$.

Based on Case 1 - Case 6, we can write the distance function of any two vertices in the following: $d(x_{i,j}x_{k,l}) = \begin{cases} |j-l| & \text{if } i = k \\ |i-k| + |j-l| & \text{if } i \neq k. \end{cases}$ For illustration of the resolving independent dominating set can be seen in Figure 5. The distance representation of the graph $G_{5,3}$ can be written in Table 2.

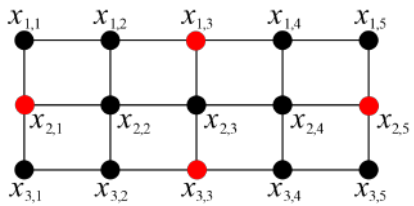

Figure 5. The Illustration of resolving independent dominating set of $G_{5,3}$

Table 2. The distance reresentation $x_{i,j} \in G_{5,3}$ to $W = \{x_{1,3}, x_{2,1}, x_{2,5}, x_{3,3}\}$

$x_{i,j}$	$r(x_{i,j}\|W)$	$x_{i,j}$	$r(x_{i,j}\|W)$
$x_{1,1}$	$(2,1,4,5)$	$x_{2,4}$	$(2,3,1,2)$
$x_{1,2}$	$(1,2,4,3)$	$x_{2,5}$	$(3,4,0,3)$
$x_{1,3}$	$(0,3,3,2)$	$x_{3,1}$	$(4,1,5,2)$
$x_{1,4}$	$(1,4,2,3)$	$x_{3,2}$	$(3,2,4,1)$
$x_{1,5}$	$(2,5,1,4)$	$x_{3,3}$	$(2,3,3,0)$
$x_{2,1}$	$(3,0,4,3)$	$x_{3,4}$	$(3,4,3,1)$
$x_{2,2}$	$(2,1,3,2)$	$x_{3,5}$	$(4,5,1,2)$
$x_{2,3}$	$(1,2,2,1)$		

3.2. The Application of Resolving Dominating Independent Set

The subsequent research result pertains to the implementation of Resolving Independent Dominating Sets in the context of precision agriculture. From now on, we will do time series forecasting on the precision agriculture dataset, namely, the Relative Humidity (RH) and CO_2 concentration of coffee agroforestry. The dataset is obtained from the simulation of placing the smart sensor for Relative Humidity (RH) and CO_2 concentration. The placement

of those sensors with respect to the planting design is derived from Theorem 4. The number of Relative Humidity (RH) and Carbon Dioxide (CO_2) sensors is equal to the obtained resolving independent domination number $\gamma_{ri}(G_{m,n})$.

To implement RIDS for shade tree placement and its application to STGNN multi-step forecasting on RH and CO_2 concentration of coffee agroforestry, we follow the following steps: (1) Capture coffee agroforestry map using Google Earth App, (2) Design a planting layout of coffee agroforestry (3) Determine RA and RRA using DepthmapX (4) Place shading trees using RIDS (5) Choose two smart sensors (6) Assemble the smart sensors (7) Write an Arduino IDE program (8) Place the smart sensors on the shading trees (9) Create Thinkspeak Channel (10) Collect the Thinkspeak data output (11) Convert RH and CO_2 data on Excel, (12) Run STGNN programming for data training and testing (13) Observe the performance of STGNN on the MSE, RMSE MAE, Accuracy, R2, (14) Compare the performance between several Models. For details, see Figure 6.

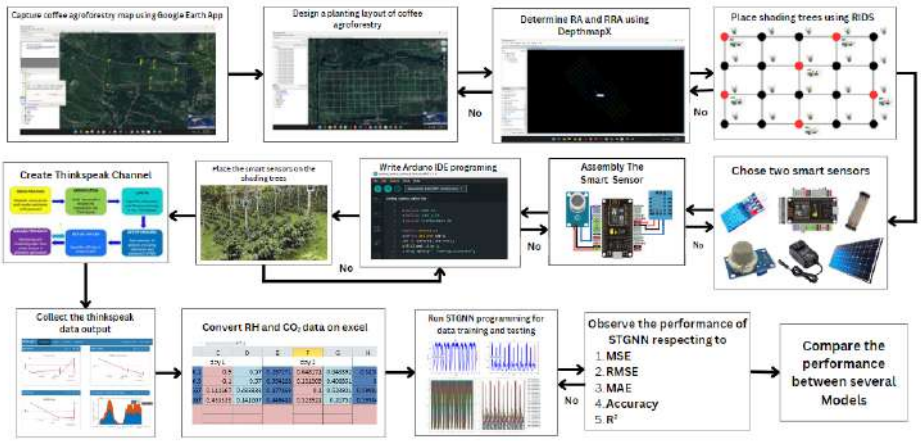

Figure 6. Conceptual Framework Design for Implementing RIDS in Precision Agriculture

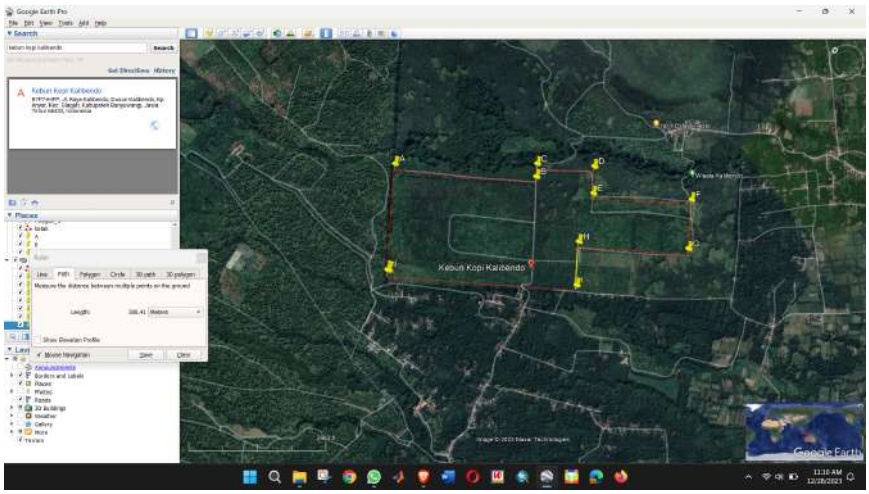

Figure 7. Coffee Agroforestry of Kalibendo Coffee Plantation, Banyuwangi Regency

The initial step is to identify the coffee plantation's location. The chosen location is Kalibendo Coffee Plantation, Banyuwangi Regency, which covers an area of 599 m^2. To facilitate the planting layout, we captured images of the land using the Google Earth App, as shown in Figure 7. Subsequently, we designed the planting layout on the land

using a grid. The outcome of the planting layout is visible in Figure 8. The results from Figure 8 were converted to an SHP file for RA and RRA analysis using the DepthmapX application. The results of the analysis can be observed in Figure 9.

Figure 8. Illustration of the Coffee Agroforestry Layout at Kalibendo Plantation in a Grid Format (Planting Design 1).

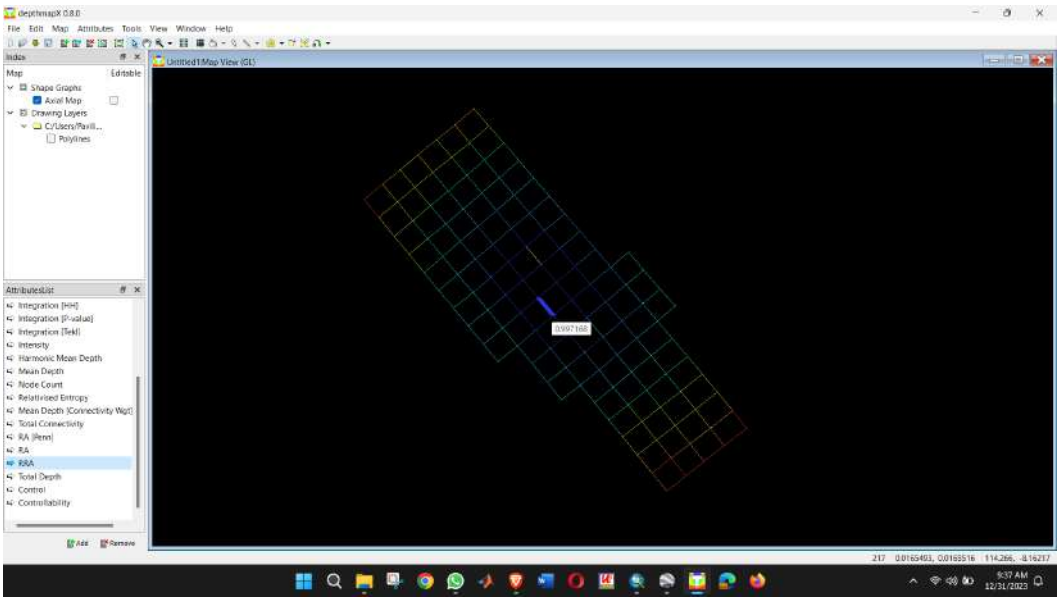

Figure 9. The Illustration of Coffee Agroforestry on Grid

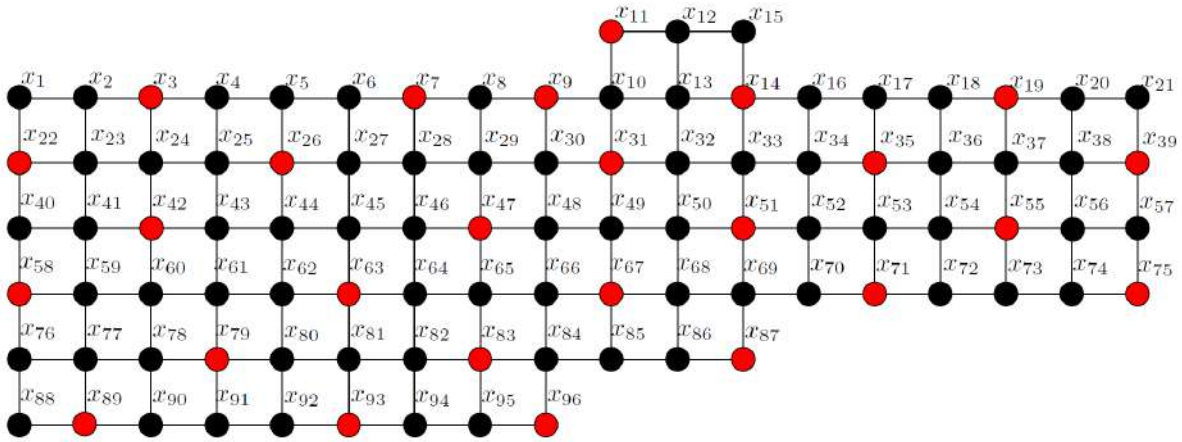

Figure 10. Sensor Placement in Shading Trees using RIDS

The Figure 9 shows that the epicentre in the coffee plantation area has the smallest RRA value of 0.997168, indicating the easiest access to each point. Therefore, the monitoring centre of the coffee plantation is located there. Next, we apply RIDS to lay shading trees, as shown in Figure 10. Smart sensors are placed in each shading tree. To facilitate understanding for readers from agricultural domains, Table 3 presents a mapping between the graph components used in this study and their real-world counterparts in coffee agroforestry systems.

Table 3. Mapping between graph components and real-world counterparts in coffee agroforestry systems

Graph Component	**Symbol**	**Real-World Counterpart**	**Description**
Vertex Set	$V(G)$	Shade Tree Locations / Sensor Nodes	Each vertex represents a location where a shade tree is planted or a sensor is placed.
Edge Set	$E(G)$	Adjacency / Spatial Proximity	An edge exists if two shade trees (or sensors) are considered adjacent based on spatial criteria (e.g., within 3 meters).
Independent Dominating Set	$D \subseteq V(G)$	Optimal Subset of Shade Trees	A subset of shade trees that efficiently covers the entire agroforestry area, ensuring no two selected trees are adjacent.
Resolving Independent Dominating Set	$W \subseteq D$	Optimal Monitoring Points (Sensor Placement)	A selected subset of D used for sensor deployment to enable unique identification of microclimatic conditions.
Adjacency Matrix	A	Matrix of Shade Tree Adjacency	A binary matrix representing which trees are adjacent (connected).
Modified Adjacency Matrix	$B = A + I$	Self-loop Enhanced Adjacency	Adds self-loops to allow each sensor to include its own readings during message passing in GNN.

In addition to the Kalibendo grid-based layout, we also conducted a comparison using an alternative planting layout from a different location, namely the Arabica Sidomulyo agroforestry system. This layout, which features a more irregular and heterogeneous tree arrangement, is illustrated in Figure 11. This comparison was conducted to evaluate the generalizability and robustness of the proposed method across different agroforestry configurations.

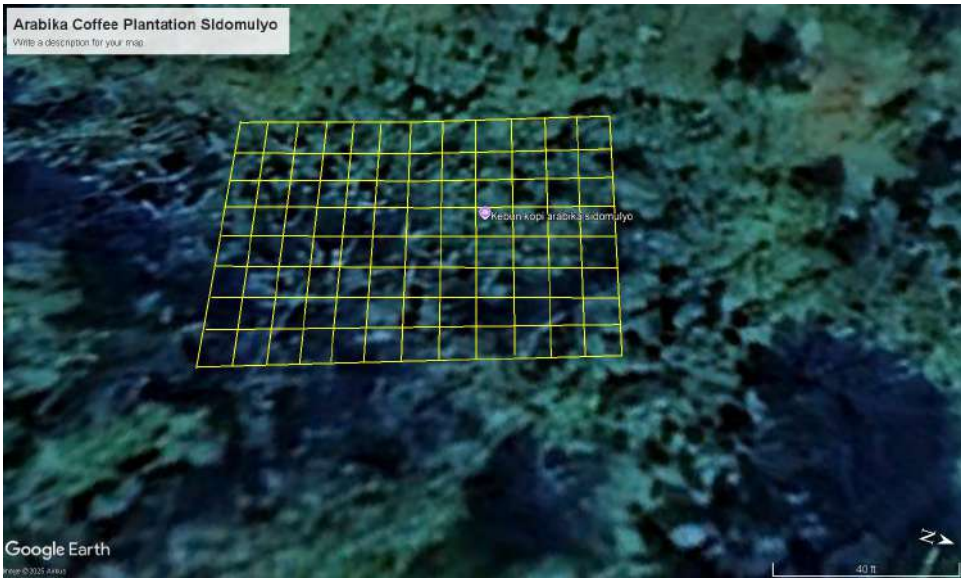

Figure 11. Illustration of the coffee agroforestry layout at Arabica Sidomulyo Plantation in a grid format (Planting Design 2).

3.3. Numerical Analysis and Programming Simulation

We will now discuss the results of the programming simulation. Prior to showing the results, we will describe the numerical analysis. We first show analytically the embedding process of vertex features and the Resolving Independent Dominating Sets of a specific graph, see Observation 1. Lastly, we use collected data to train and test the STGNN model for multi-step time series forecasting of the RH and CO_2 concentration in coffee agroforestry. We split the dataset into two sets, namely 70% of training data and 30% of testing data.

To support model transparency and reproducibility, we provide a schematic representation of the Graph Convolutional Network (GCN) architecture used in this study, as shown in Figure 12. The model consists of two GCN layers, where the first layer generates a 32-dimensional embedding with ReLU activation, followed by a dropout layer to prevent overfitting. The second GCN layer reduces the embedding to 16 dimensions, which are then passed to the output layer to compute node classification scores or sensor placement priorities. The adjacency matrix is formulated as $B = A + I$, incorporating self-loops to allow each node to retain its own feature information during the message passing phase.

The hyperparameters used for training the model are listed in Table 4. These values were selected empirically to balance performance and generalization, particularly in the context of a small sensor network graph within a coffee agroforestry system. The node embedding dimension of 32 in the first layer provides expressive capacity while remaining computationally efficient.

Table 4. Hyperparameters used in the GCN model

Parameter	**Value**
Number of GCN Layers	2
Node Embedding Dimensions	32 (Layer 1), 16 (Layer 2)
Activation Function	ReLU
Dropout Rate	0.3
Optimizer	Adam
Learning Rate	0.001
Number of Epochs	200
Batch Size	Full-batch

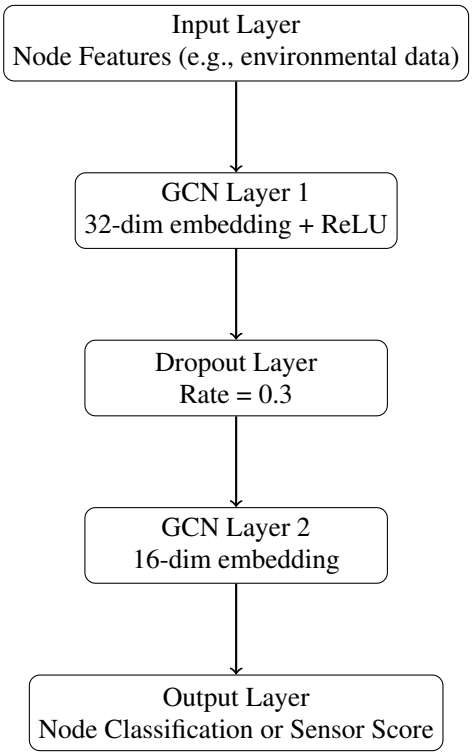

Figure 12. Graph Convolutional Network (GCN) architecture for node-level prediction and sensor selection in coffee agroforestry systems.

Observation 1
Let G be a graph with order n. Assume the vertex and edge sets are defined as $V(G) = \{v_1, v_2, \ldots, v_{n-1}, v_n\}$ and $E(G) = \{v_i v_j | v_i, v_j \in V(G)\}$, respectively. Let the vertex features be represented by the matrix $h_{v_i} = \begin{bmatrix} s_{1,1} & s_{1,2} & \cdots & s_{1,m} \\ s_{2,1} & s_{2,2} & \cdots & s_{2,m} \\ \vdots & \vdots & \ddots & \vdots \\ s_{n,1} & s_{n,2} & \cdots & s_{n,m} \end{bmatrix}$. The embedding of a vertex is computed through message passing from its neighboring vertices as $h_v^{l+1} = AGG\{m_u^{l+1}, u \in N(v)\}$ using the aggregation function $\mathbf{sum}(\cdot)$, where $l = 0, 1, 2, 3, \ldots, k$. Hence, $h_v^{l+1} = SUM\{m_u^{l+1}, u \in N(v)\}$ based on the matrix $B = A + I$, with A being the adjacency matrix and I the identity matrix.

Proof. By graph G, we can determine the matrix adjacency A. Since, we need to consider the self adjacency for each vertex of G, we need to add A by identity matrix I and we have matrix B as follow.

$$B = A + I = \begin{bmatrix} b_{1,1} & b_{1,2} & \cdots & b_{1,n} \\ b_{2,1} & b_{2,2} & \cdots & b_{2,n} \\ \vdots & \vdots & \ddots & \vdots \\ b_{n,1} & b_{n,2} & \cdots & b_{n,n} \end{bmatrix}$$

According to the single layer GNN algorithm, we need to initialize the learning weight matrix as follow.

$$W = \begin{bmatrix} w_{1,1} & w_{1,2} & \cdots & w_{1,m} \\ w_{2,1} & w_{2,2} & \cdots & w_{2,m} \\ \vdots & \vdots & \ddots & \vdots \\ w_{m,1} & w_{m,2} & \cdots & w_{m,m} \end{bmatrix}$$

The assigned weight is utilized to compute the value of m_{v_i} and will also serve as the updated weight in the subsequent iteration. The vertex embedding process in Graph Neural Networks (GNNs) consists of two primary stages: *message passing* and *aggregation*. During the initial phase, message passing is performed through the function $\mathbf{m_u} = MSG(h_u)$. When using a linear transformation layer, this becomes $\mathbf{m_u}^{l+1} = W^l \cdot h_u^l$, where $l = 0, 1, 2, \ldots, k$. The iterative computation process can thus be initiated as follows:

$$m_{v_i}^1 = H_{v_i}^0 \cdot W^0 = \begin{bmatrix} s_{1,1} & s_{1,2} & \cdots & s_{1,m} \\ s_{2,1} & s_{2,2} & \cdots & s_{2,m} \\ \vdots & \vdots & \ddots & \vdots \\ s_{n,1} & s_{n,2} & \cdots & s_{n,m} \end{bmatrix} \times \begin{bmatrix} w_{1,1} & w_{1,2} & \cdots & w_{1,m} \\ w_{2,1} & w_{2,2} & \cdots & w_{2,m} \\ \vdots & \vdots & \ddots & \vdots \\ w_{m,1} & w_{m,2} & \cdots & w_{m,m} \end{bmatrix}$$

$$= \begin{bmatrix} s_{1,1} \times w_{1,1} + \cdots + s_{1,m} \times w_{m,1} & \cdots & s_{1,1} \times w_{1,m} + \cdots + s_{1,m} \times w_{m,m} \\ s_{2,1} \times w_{1,1} + \cdots + s_{2,m} \times w_{m,1} & \cdots & s_{2,1} \times w_{1,m} + \cdots + s_{2,m} \times w_{m,m} \\ \vdots & \ddots & \vdots \\ s_{n,1} \times w_{1,1} + \cdots + s_{n,m} \times w_{m,1} & \cdots & s_{n,1} \times w_{1,m} + \cdots + s_{n,m} \times w_{m,m} \end{bmatrix}$$

After completing the message passing phase, the process proceeds to the second stage: *aggregation*, which focuses on the neighborhood of vertex v. Using an aggregation function such as $\mathbf{sum}(\cdot)$, the node representation is updated according to the rule

$$h_v^{l+1} = AGG\left\{m_u^{l+1} \mid u \in N(v)\right\}.$$

Specifically, when using summation as the aggregation operator, we have

$$h_v^{l+1} = \sum_{u \in N(v)} m_u^{l+1}.$$

With respect to the matrix formulation where $B = A + I$ (the adjacency matrix plus identity), the updated embedding vector for node v_i at layer $l = 1$, denoted $h_{v_i}^1$, can be expressed as follows:

$$h_{v_i}^{l+1} = \begin{bmatrix} m_{v_{1,1}}^{l+1} & m_{v_{1,2}}^{l+1} & \cdots & m_{v_{1,m}}^{l+1} \\ m_{v_{2,1}}^{l+1} & m_{v_{2,2}}^{l+1} & \cdots & m_{v_{2,m}}^{l+1} \\ \vdots & \vdots & \ddots & \vdots \\ m_{v_{n,1}}^{l+1} & m_{v_{n,2}}^{l+1} & \cdots & m_{v_{n,m}}^{l+1} \end{bmatrix}$$

The next step involves calculating the error value, which quantifies the proximity between two adjacent vertices within the embedding space. A lower error indicates a shorter distance between the embeddings of the connected vertices. This error can be defined mathematically as:

$$\text{error}^l = \frac{\left\|h_{v_i} - h_{v_j}\right\|_\infty}{|E(G)|}, \quad \text{where } i, j \in \{1, 2, \ldots, n\}.$$

We then evaluate whether the condition error $\leq \epsilon$ is satisfied. If not, the weight matrix W^l must be updated using the previous embedding $h_{v_i}^l$. The update rule for the learning weight matrix is given by:

$$W^{l+1} = W^l + \alpha \cdot \text{error}^l \cdot (h_{v_i}^l)^T \cdot h_{v_i}^{l+1},$$

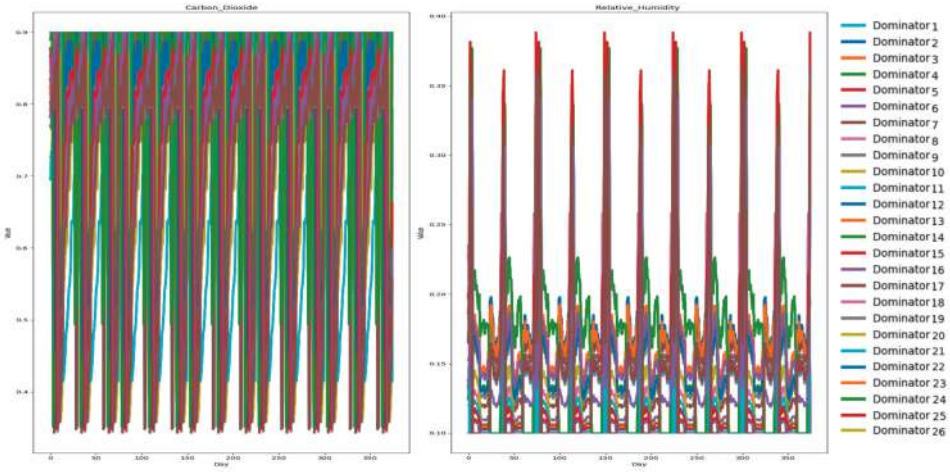

Figure 13. Distribution of RH and CO2

and this process is repeated until the error value falls below the threshold ϵ. □

The implementation of the Single-Layer Graph Neural Network (SLGNN) algorithm enables the development and execution of programming to analyse the concentration of relative humidity and carbon dioxide in the context of coffee agroforestry systems. First, we collected some data from the smart sensors of RH and CO_2 within 62 days observations. We developed the STGNN programming to train 70% input data, test 30% input data and finally forecast the RH and CO_2 concentration for several days ahead. Figure 13 shows the data distribution for 6 days.

In regards with the algorithm above, we need to deal with node embedding along with 26 agroforestry. This embedding process converted the original feature of three dimensions into one dimension by using message passing and an aggregation technique. In the message passing process, we assume that each node has some information and sends that information to its neighbours. Thus, in this process we consider the adjacency matrix including the loop of each node. Thus, instead of considering the adjacency matrix P, we consider the adjacency matrix Q = P + I. Following the steps of the above algorithm, we obtained the time series data, which is ready for analysis by using STGNN. To consider how effective the result of the node embedding, we asses the closeness of their nodes in the original networks and the embedding space. We determine the error by considering each pair of adjacent nodes by using an infinity norm. Later, we develop STGNN multi-step time series forecasting to train 70% of the data and obtain the smallest Root Mean Square Error (RMSE) or Mean Square Error (MSE) of the testing data.

To convince the robustness of the STGNN model, we compared six models, namely Historical Average (HA), Auto Regressive Integrated Moving Average (ARIMA), Support Vector Regression (SVR), Graph Convolutional Networks (GCN), Gated Recurrent Unit (GRU), and Spatio-Temporal Graph Neural Networks (STGNN). The comparison results between these models can be seen in Figure 14 and Table 5, based on Dataset 1, which was derived from a structured planting design with uniform shading tree distribution. Figure 14 shows that STGNN needed approximately 200 epochs to reach the lowest error, with a stable convergence pattern and minimal oscillation compared to other models. The superior performance of STGNN was consistently reflected by various metrics, including RMSE, MAE, accuracy, and the coefficient of determination (R^2), especially in forecasting 5, 10, 15, and 20 days ahead. Based on these results, we conclude that STGNN is capable of accurately forecasting and monitoring 26 agroforestry sensor points in this layout, using the Resolving Independent Dominating Sets concept to minimise sensor deployment.

To validate the representativeness of the selected nodes, we conducted a one-way ANOVA test comparing RH and CO_2 values across RIDS and non-RIDS nodes. The results ($p > 0.05$) indicate no statistically significant difference, suggesting that the selected nodes adequately capture environmental variability across the plantation.

To further examine the model's generalizability across different agroforestry conditions, we conducted the same comparative experiment on Dataset 2, which represents a heterogeneous planting design with irregular tree

Table 5. The prediction results of the T-GCN model and other baseline methods on Dataset 1 (Planting Design 1)

T	Metric	HA	ARIMA	SVR	GCN	GRU	STGNN
5 Days	RMSE	7.7087	8.0051	7.1357	8.1706	4.0081	3.3051
	MAE	5.2856	6.0092	4.9165	7.2225	2.2303	2.2061
	Accuracy	0.6706	0.1378	0.6871	0.6123	0.4068	0.5106
	R^2	0.2324	0.0372	0.6101	0.4037	0.7437	0.7531
10 Days	RMSE	7.7087	8.1212	7.4736	9.1130	4.0667	3.8606
	MAE	5.4836	6.1141	4.8719	7.1101	2.5006	2.5541
	Accuracy	0.5406	0.4231	0.6856	0.5305	0.7141	0.7115
	R^2	0.6824	0.0712	0.6131	0.5086	0.8344	0.7413
15 Days	RMSE	7.6087	8.1101	7.4633	9.2021	4.0002	3.7740
	MAE	5.2758	6.1141	5.0121	7.3204	2.4007	2.2355
	Accuracy	0.4506	0.3160	0.5975	0.5373	0.5032	0.4143
	R^2	0.7224	0.0716	0.8111	0.2027	0.7350	0.8109
20 Days	RMSE	7.7077	8.2031	7.4371	9.4303	4.1101	4.0021
	MAE	5.4448	6.2107	5.0503	7.3110	2.7311	2.5778
	Accuracy	0.5606	0.3172	0.5771	0.5155	0.6015	0.5028
	R^2	0.6524	0.0714	0.7141	0.5822	0.7620	0.7702

Table 6. The prediction results of the T-GCN model and other baseline methods on Dataset 2 (Planting Design 2)

T	Metric	HA	ARIMA	SVR	GCN	GRU	STGNN
5 Days	RMSE	7.8201	8.1123	7.3050	8.2214	4.0507	3.4003
	MAE	5.3120	6.0845	4.9822	7.3010	2.2785	2.1810
	Accuracy	0.6580	0.1292	0.6734	0.6015	0.4187	0.5288
	R^2	0.2203	0.0254	0.6020	0.3951	0.7412	0.7629
10 Days	RMSE	7.8333	8.2305	7.5088	9.2507	4.1051	3.9308
	MAE	5.5329	6.1890	4.9244	7.2294	2.5521	2.4976
	Accuracy	0.5253	0.4104	0.6705	0.5230	0.7010	0.7239
	R^2	0.6675	0.0658	0.6009	0.4953	0.8265	0.7487
15 Days	RMSE	7.6908	8.1898	7.5041	9.3400	4.0754	3.8205
	MAE	5.3182	6.1345	5.0340	7.3922	2.4519	2.2683
	Accuracy	0.4395	0.2993	0.5823	0.5242	0.4972	0.4281
	R^2	0.7092	0.0629	0.8005	0.1892	0.7210	0.7991
20 Days	RMSE	7.8156	8.3112	7.4795	9.5108	4.1958	4.1113
	MAE	5.4911	6.2804	5.0730	7.3803	2.7815	2.6211
	Accuracy	0.5454	0.3025	0.5632	0.5020	0.5984	0.5193
	R^2	0.6380	0.0611	0.7038	0.5682	0.7543	0.7658

spacing and microclimatic variation. The results, presented in Table 6, show that STGNN again outperformed baseline models across all forecast horizons, despite slightly fluctuating performance values due to environmental complexity. This reinforces the model's adaptability and robustness across varying field layouts. Consequently, the findings suggest that the proposed STGNN framework is not only effective in uniform agroforestry systems but also scalable and generalizable to more complex, real-world plantation configurations.

In addition to its superior forecasting accuracy, the STGNN model offers structural advantages by combining spatial and temporal learning. The spatial structure, derived from tree adjacency graphs, enables the model to consider interactions between neighbouring plants, while the temporal component—via recurrent layers—captures evolving trends in environmental variables. This contrasts with classical models such as ARIMA, which rely solely on temporal autoregression and ignore spatial dependencies, limiting their capacity to model agroforestry systems with complex spatial heterogeneity.

Nevertheless, the STGNN framework is not without limitations. Its reliance on graph structures and multi-step temporal encoding leads to higher computational demands compared to traditional models. Furthermore, performance may be sensitive to missing or corrupted sensor data, particularly when such data is associated with nodes of high connectivity. These factors should be considered when deploying the model in resource-constrained environments or in systems with sparse sensor coverage.

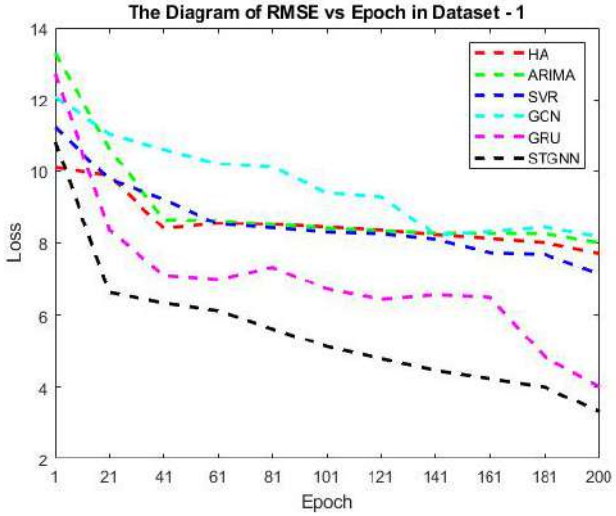

Figure 14. Comparison of predicted performance

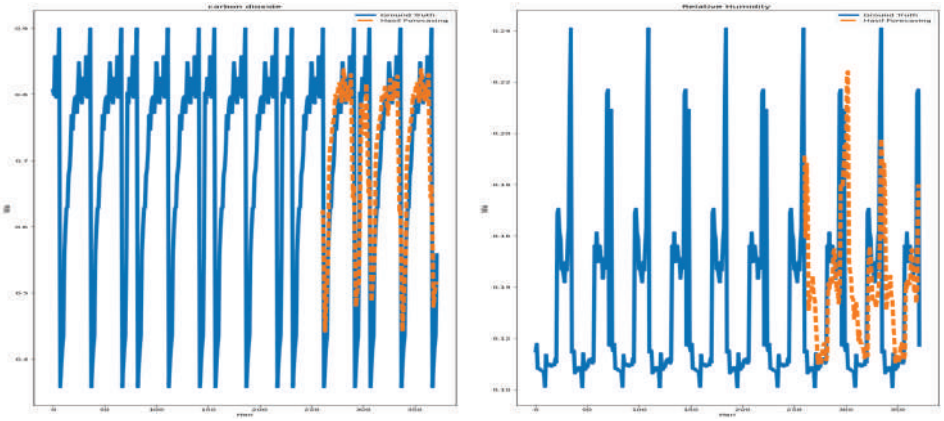

Figure 15. Training and Testing Process of RH and CO_2

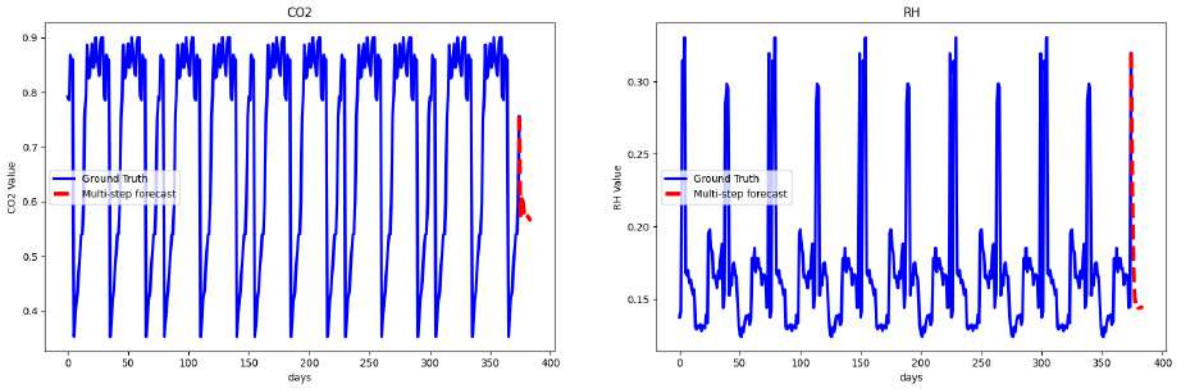

Figure 16. Multi-Step Time Series Forecasting on RH and CO_2 for 10 Days Ahead

4. Conclusion

In this paper, we have studied the Resolving Independent Dominating Sets (rids) of a specific family of graphs, namely $C_m \triangleright P_n$, and $G_{n,m}$. We have shown that the local (a, d)-edge chromatic numbers of the two graphs attain the best lower bound. However, since this study is considered to be a NP-hard problems, finding the exact value of $\gamma_{ri}(G)$ is still widely open. Thus, we propose the open problem: Find the exact values of the Resolving Independent Domination number of other specific family of graphs and their operations. Apply the results for shade tree placement and for STGNN multi-step forecasting on Controlled Environment Agriculture (CEA) in a smart agroforestry.

Acknowledgement

We gratefully acknowledge LP2M University of Jember, PUI-PT Combinatorics and Graph, CGANT University of Jember for their excellent collaboration and support for finishing this study in the year 2025.

REFERENCES

1. Bosselmann, A. S., Dons, K., Oberthur, T., Olsen, C. S., Ræbild, A., & Usma, H. (2009). The influence of shade trees on coffee quality in small holder coffee agroforestry systems in Southern Colombia. *Agriculture, Ecosystems & Environment*, 129(1-3), 253-260.
2. Nesper, M., Kueffer, C., Krishnan, S., Kushalappa, C. G., & Ghazoul, J. (2017). Shade tree diversity enhances coffee production and quality in agroforestry systems in the Western Ghats. *Agriculture, Ecosystems & Environment*, 247, 172-181.
3. Lalany, B., Lanza, G., Leiva, B., Mercado, L., & Haggar, J. (2023). Shade versus intensification: Trade-off or synergy for profitability in coffee agroforestry systems? *Agricultural Systems*, 214, 103814, doi:10.1016/j.agsy.2023.103814
4. Sun, H., Zhang, F., Raza, S. T., Zhu, Y., Ye, T., Rong, L., & Chen, Z. (2023). Three decades of shade trees improve soil organic carbon pools but not methane uptake in coffee systems. *Journal of Enviromental Management*, 347, 119166, doi:10.1016/j.jenvman.2023.119166
5. Schnabel, F., de Melo Virginio Filho, E., Xu, S., Fisk, I. D., Roupsard, O., & Haggar, J. (2018). Shade trees: a determinant to the relative success of organic versus conventional coffee production. *Agroforestry systems*, 92, 1535-1549.
6. Berry, R., Livesley, S. J., & Aye, L. (2013). Tree canopy shade impacts on solar irradiance received by building walls and their surface temperature. *Building and environment*, 69, 91-100.
7. Lara-Estrada, L., Rasche, L., & Schneider, U. A. (2023). Exploring the cooling effect of shading for climate change adaptation in coffee areas. *Climate Risk Management*, 42, 100562.
8. Akbari, H. (2002). Shade trees reduce building energy use and CO2 emissions from power plants. *Environmental pollution*, 116, S119-S126.
9. Abou Rajab, Y., Leuschner, C., Barus, H., Tjoa, A., & Hertel, D. (2016). Cacao cultivation under diverse shade tree cover allows high carbon storage and sequestration without yield losses. *PloS one*, 11(2), e0149949.
10. Tscharntke, T., Clough, Y., Bhagwat, S. A., Buchori, D., Faust, H., Hertel, D., & Wanger, T. C. (2011). Multifunctional shade-tree management in tropical agroforestry landscapes–a review.*Journal of Applied Ecology*, 48(3), 619-629.
11. Schooler, S. L., Johnson, M. D., Njoroge, P., & Bean, W. T. (2020). Shade trees preserve avian insectivore biodiversity on coffee farms in a warming climate. Ecology and evolution, 10(23), 12960-12972.
12. Piato, K., Lefort, F., Subía, C., Caicedo, C., Calderón, D., Pico, J., & Norgrove, L. (2020). Effects of shade trees on robusta coffee growth, yield and quality. A meta-analysis. *Agronomy for Sustainable Development*, 40, 1-13
13. Lugo-Pérez, J., Hajian-Forooshani, Z., Perfecto, I., & Vandermeer, J. (2023). The importance of shade trees in promoting carbon storage in the coffee agroforest systems. Agriculture, Ecosystems & Environment, 355, 108594.
14. Ehrenbergerová, L., Cienciala, E., Kučera, A., Guy, L., & Habrová, H. (2015). Carbon stock in agroforestry coffee plantations with different shade trees in Villa Rica, Peru. Agroforestry Systems, 90(3), 433–445.
15. Richards, M. B., & Méndez, V. E. (2013). Interactions between Carbon Sequestration and Shade Tree Diversity in a Smallholder Coffee Cooperative in El Salvador. Conservation Biology, 28(2), 489–497. Portico.
16. Perez, J. L., Forooshani, Z. H., Perfecto, I., Vandermeer, J. (2023). The importance of shade trees in promoting carbon storage in the coffee agroforest systems. *Agriculture, Ecosystems & Environment*. Vol. 355, 108594, pp. 1-9, doi:10.1016/j.agee.2023.108594
17. Ayalew, B., Hylander, K., Zewdie, B., Shimales, T., Adugna, G., Mendesil, E., Nemomissa, S., & Tack, A. J. M. (2022). The impact of shade tree species identity on coffee pests and diseases. *Agriculture, Ecosystems and Environment*. Vol. 340, 108152, pp. 1-14, doi: 10.1016/j.agee.2022.108152
18. Mursyidah, I. L., Dafik, Kristiana, A. I., Agustin, I. H., Maylisa, I. N., & Alfarisi, R. (2023). On Rainbow Antimagic Coloring of Some Classes of Graphs. *Proceedings of the 6th International Conference of Combinatorics, Graph Theory, and Network Topology (ICCGANT 2022)*, pp. 73-93, doi:10.2991/978-94-6463-138-8_8
19. Santoso, K. A., Mursyidah, I. L., Agustin, I. H., Dafik, Venkatraman, S., & Venkatachalam, M. (2025). A Robust Algorithm for Asymmetric Cryptography Using Rainbow Vertex Antimagic Coloring. *Statistics, Optimization & Information Computing*, 13(5), 1984-1999.

20. Dafik, D., Nisviasari, R., Agustin, I. H., Humaizah, R., Wardani, D. A. R., & Venkatachalam, M. (2023, May). On resolving strong domination number of several graph classes. *AIP Conference Proceedings, AIP Publishing*. Vol. 2718 (1), doi:10.1063/5.0137788
21. Febrinanto, F. G., Xia, F., Moore, K., Thapa, C., & Aggarwal, C. (2023). Graph lifelong learning: A survey. IEEE Computational Intelligence Magazine, 18(1), 32-51.
22. Haynes, T. W., Hedetniemi, S. T., & Henning, M. A. (Eds.). (2020). Topics in domination in graphs (Vol. 64). Cham: Springer.
23. Chen J S., Hung R W., Kohjerdi, F K., & Huang Y F. (2022). Domination and Independent Domination in Extended Supergrid Graphs. *Algorithms,* 15(11), 402. https://doi.org/10.3390/a15110402
24. Shaheen, R. (2019). On independent domination numbers of grid and toroidal grid directed graphs. *Communications in Combinatorics and Optimization,* 4(1), pp. 71-77. DOI: 10.22049/CCO.2019.26282.1090
25. Febrinanto, F. G., Moore, K., Thapa, C., Liu, M., Saikrishna, V., Ma, J., & Xia, F. (2023). Entropy Causal Graphs for Multivariate Time Series Anomaly Detection. arXiv preprint arXiv:2312.09478.
26. Febrinanto, F. G., & Nisviasari, R. (2021). The implementation of Blockchain framework in MOOCs to support a freedom of learning in Indonesia. In Journal of Physics: Conference Series (Vol. 1836, No. 1, p. 012043). IOP Publishing.
27. Mazidah, T., Dafik, Slamin, Agustin, I. H., & Nisviasari, R. (2020). Resolving independent domination number of some special graphs. *J. Phys.: Conf. Ser.* **1832** 012002. doi:10.1088/1742-6596/1832/1/012022
28. Prihandini, R. M., Az-Zahra, N. A., Dafik, Prihandoko, A. C., & Adawiyah, R. (2023). Resolving Independent Dominating Set of Flower, Gear, and Sunflower Graph. *Contemporary Mathematics and Applications*. 5(2), pp. 64-78.
29. Hou, M., Ren, J., Febrinanto, F., Shehzad, A., & Xia, F. (2021), December). Cross network representation matching with outliers. In 2021 International Conference on Data Mining Workshops (ICDMW) (pp. 951-958). IEEE.
30. Yu, S., Xia, F., Wang, Y., Li, S., Febrinanto, F. G., & Chetty, M. (2022). PANDORA: Deep Graph Learning Based COVID-19 Infection Risk Level Forecasting. IEEE Transactions on Computational Social Systems.
31. F. G., Liu, M., & Xia, F. (2023). Balanced Graph Structure Information for Brain Disease Detection. In Pacific Rim Knowledge Acquisition Workshop (pp. 134-143). Singapore: Springer Nature Singapore.
32. Wang, L., Yu, S., Febrinanto, F. G., Alqahtani, F., & El-Tobely, T. E. (2022). Fairness-Aware Predictive Graph Learning in Social Networks. Mathematics, 10(15), 2696.
33. Muklisin, A., Tirta, I. M., Dafik, Baihaki, R. I., & Kristiana, A. I. (2023). The Analysis of Airport Passengers Flow by Using Spatial Temporal Graph Neural Networks and Resolving Efficient Dominating Set. *Proceedings of the 1st International Conference on Neural Networks and Machine Learning 2022 (ICONNSMAL 2022)*. pp. 3-20. doi:10.2991/978-94-6463-174-6_2
34. Harliyuni, A. D., Dafik, Slamin, Ridlo, Z. R., Alfarisi, R. (2023). On the Spatial Temporal Graph Neural Network Analysis Together with Local Vertex Irregular Reflexive Coloring for Time Series Forecasting on Passenger Density at Bus Station. *Proceedings of the 1st International Conference on Neural Networks and Machine Learning 2022 (ICONNSMAL 2022)*. pp. 305-323, doi:10.2991/978-94-6463-174-6_22
35. Mufidati, D., Ridlo, Z. R., Slamin, Maylisa, I. N., Dafik. (2023). On Time Series Forecasting Analysis of Soil Moisture by Using Artificial Neural Networks Based - on Rainbow Antimagic Coloring for Autonomous Irrigation System on Horizontal Farming. *Proceedings of the 1st International Conference on Neural Networks and Machine Learning 2022 (ICONNSMAL 2022)*, pp. 234-256, doi:10.2991/978-94-6463-174-6_18
36. Mauliska, N., Lestari, W., Wisudaningsih, E. T., & Islam, M. H. (2023). Application of Spatial Temporal Graph Neural Networks for Forecasting Data Time Series River Pollution Waste Content in Probolinggo. *Proceedings of the 1st International Conference on Neural Networks and Machine Learning 2022 (ICONNSMAL 2022)*, pp. 257-272, doi:10.2991/978-94-6463-174-6_19
37. Mursyidah, I. L., Agustin, I. H., Baihaki, R. I., Febrinanto, F. G., Husain, S. K. B. S., & Sunder, R. (2024). On Rainbow Vertex Antimagic Coloring and Its Application on STGNN Time Series Forecasting on Subsidized Diesel Consumption. *IAENG International Journal of Applied Mathematics*, 54(5), 984-996.
38. Kristiana, A. I., Rachmasari, E., Dafik, Agustin, I. H., Mursyidah, I. L., & Alfarisi, R. (2024). On b-Coloring Analysis of Graphs: An Application to Spatial-Temporal Graph Neural Networks for Multi-Step Time Series Forecasting of Soil Moisture and pH in Companion Farming. *European Journal of Pure and Applied Mathematics*, 17(4), 3356-3369.